

VLF/LF Intracloud lightning height determination

D. A. Smith, M. J. Heavner, A. R. Jacobson, X. M. Shao, R. S. Massey, R. J. Sheldon,

K. C. Wiens

Los Alamos National Laboratory

Short title: VLF/LF INTRACLOUD LIGHTNING HEIGHT DETERMINATION

Abstract. The Los Alamos Sferic Array (LASA) recorded VLF/LF electric-field-change signals from over ten million lightning discharges during the period from 1998 to 2001. Using the differential-times-of-arrival of lightning sferics recorded by three or more stations, the latitudes and longitudes of the source discharges were determined. Under conditions of favorable geometry and ionospheric propagation, sensors obtained ionospherically reflected skywave signals from the lightning discharges in addition to the standard groundwave sferics. In approximately 1% of all waveforms, automated processing identified two 1-hop skywave reflection paths with delays indicative of an intracloud (height greater than 5 km) lightning source origin. For these events it was possible to determine both the height of the source above ground and the virtual reflection height of the ionosphere. Ionosphere heights agreed well with published values of 60 to 95 km with an expected diurnal variation. Source height determinations for 100,000+ intracloud lightning events ranged from 7 to 20 km AGL with negative-polarity events occurring above ~ 15 km and positive-polarity events occurring below ~ 15 km. Approximately 100 of the intracloud events with LASA height determinations were also recorded by VHF receivers on the FORTE satellite. Independent FORTE source height estimates based on delays between direct and ground-reflected radio emissions showed excellent correlation with the VLF/LF estimates, but with a +1 km bias for the VLF/LF height determinations.

Introduction

Energetic intracloud (IC) discharges are isolated lightning events that occur in thunderstorms and produce both very powerful HF/VHF radiation and distinctive narrow bipolar electric field change pulses. Initial ground-based observations of these events were published by Krider *et al.* [1975]; LeVine [1980]; Willett *et al.* [1989]; Medelius *et al.* [1991]. The discharges have been a topic of heightened interest in recent years, having been studied by the Blackbeard satellite payload [Holden *et al.*, 1995; Massey and Holden, 1995; Massey *et al.*, 1998], the FORTE satellite [Jacobson *et al.*, 1999, 2000], the New Mexico Tech Lightning Mapping Array (LMA) [Rison *et al.*, 1999], the Los Alamos Sferic Array (LASA) [Smith *et al.*, 2002], and other ground-based broadband receiving systems [Smith, 1998; Smith *et al.*, 1999a, b].

Energetic ICs (or EICs), as the discharges will be referred to in this paper, have previously been referred to as compact intracloud discharges (CIDs) [Smith, 1998; Smith *et al.*, 1999b], energetic bipolars [Krehbiel, private communications], and bipolar events [Rison *et al.*, 1999]. Their low frequency and high frequency emissions have also been given a variety of monikers. The field change waveforms were described by Willett *et al.* [1989] as narrow positive and narrow negative bipolar pulses (NPBPs and NNBPBs). EIC VHF emissions, when recorded from space along with a ground reflection, were dubbed transionospheric pulse pairs (TIPPs) by Holden *et al.* [1995].

Terminology notwithstanding, energetic ICs are distinguished from other lightning events by several noteworthy characteristics, including the following: 1. The discharges

are the most powerful source of lightning radiation in the HF and VHF radio bands [LeVine, 1980; Willett *et al.*, 1989; Holden *et al.*, 1995; Massey and Holden, 1995; Smith *et al.*, 1999a; Jacobson *et al.*, 1999; Rison *et al.*, 1999; Jacobson and Shao, 2001]. 2. Energetic ICs are typically isolated in time from other detectable discharges on a time scale of at least a few milliseconds, but often represent the initial event in an otherwise ‘normal’ intracloud lightning flash [Smith, 1998; Rison *et al.*, 1999; Jacobson and Light, 2002]. 3. Energetic ICs occur in both positive and negative polarities, as previously documented by Willett *et al.* [1989] and [Medelius *et al.*, 1991]. The negative-polarity events were not observed in the earlier work by Smith *et al.* [1999b], but have been observed since [Smith *et al.*, 2002] and are a topic of this paper.

The FORTE satellite and Los Alamos Sferic Array are two resources that have been utilized to study energetic ICs. This paper describes a method for determining discharge heights from multi-station electric field change data. The method is developed from one described by Smith *et al.* [1999b], which utilized the delays of ionosphere and ground reflections with respect to ground wave signals to determine source and ionosphere heights. The improved method includes consideration for spherical earth geometry and utilizes modeling of skywave reflections to determine times of arrival of sky wave signals accurately. The method is applied to hundreds of thousands of events, whereas the previous method was applied to tens of events. Also presented in this paper is a comparison of discharge heights determined by the sferic array (using VLF/LF radio emissions) and by the FORTE satellite (using VHF radio emissions, as described by Jacobson *et al.* [1999]). The comparison is made using 100 coincident

intracloud lightning events recorded during 3 years of cooperative observations. IC lightning altitudes are of interest because they provide insight about the meteorological conditions in discharge source regions. Having two largely-independent evaluations of source heights builds confidence in the height determinations and also provides validation for the two source height determination methods.

Los Alamos Sferic Array

Background

The Los Alamos Sferic Array (LASA) has been described in detail by [Smith *et al.*, 2002]. In brief, LASA is a collection of field change meters (measuring transient changes in the vertical electric field) that has been operated since May 1998 and has consisted of as many as eleven electric field change meters located at twenty locations in New Mexico, Florida, Colorado, Texas, and Nebraska. The convention used for the polarity of electric field change measurements is that a negative cloud to ground lightning discharge has an initially negative going electric field change record. The array stations record and time tag (using GPS clocks with better than 2 μ s absolute accuracy) triggered field change waveforms, 24 hours per day. Once per day the waveform time stamps from all stations are compared to identify coincidences. Coincident waveforms are transferred via the Internet to Los Alamos National Laboratory, where lightning events are located, classified, and characterized. Over seven million lightning discharges have been processed by the array during 4+ years of operation.

VLF/LF Source Height Methodology

Figure 1.

The narrow bipolar field change pulses produced by EICs are both narrow (lasting less than 20 μs) and isolated (typically by at least several hundred μs) compared to other VLF/LF emissions from lightning processes [Smith *et al.*, 1999b]. The use of bipolar as part of the descriptive terminology applied to these waveforms is much stricter than the typical use of ‘bipolar’ indicates: the direct pulse has a monopulse of each polarity with very little other contribution to the waveform. Because of these characteristics, it is often possible to unequivocally identify their VLF/LF reflections from the ionosphere and earth in the 8 ms sferic waveforms most commonly recorded by LASA. Figure 1 shows an example of a NPBP recorded by 4 array stations. Reflections are evident in each of the waveforms, which are presented in order from nearest to farthest distance between the source and the LASA receivers. Note the systematic relationship in the reflection delays as a function of range: with increasing range, the delays from the groundwave pulse to the two reflections decrease as a result of the shrinking differential path length. The geometry responsible for the VLF/LF reflection pairs is illustrated in Figure 2, which also shows the geometry for the case of VHF signals are received by a satellite from outside of the earth’s ionosphere (discussed later in this paper). Note that the polarities of the leading edge of the reflections in Figure 1 change between the ranges of ~ 150 and ~ 200 km. Both the polarity shift and range/delay relationship are better illustrated in Figure 3 which shows examples of clean sferic waveforms (not from the same discharge) recorded by sensors on different occasions (nighttime only) at

several ranges under good ionospheric conditions. The two curved lines that cross the waveforms indicate the predicted ionospheric delays for skywave reflections as a function of range for a source at a height of 12 km and an ionospheric virtual height of 86 km. The measured delays agree well with the predictions, and the leading-edge polarity reversal is evident between the ranges of 150 to 200 km.

Figure 2.

Multiple ground and ionospheric reflections of low frequency lightning sferics have previously been used to determine both the range to distant lightning return strokes and the effective reflection height of the ionosphere. Kinzer [1974] used a single sensing station and flat-earth geometry to make the source range and ionosphere height determinations from measurements of one-hop and two-hop reflection delays with respect to ground wave times of arrival. McDonald *et al.* [1979] improved and validated the Kinzer technique by introducing spherical-earth geometry and validating range determination through the use of a second sensing station. Smith [1998] and Smith *et al.* [1999b] expanded the previous techniques to permit determination of intracloud source heights for pulses with sufficiently short durations that their reflections were distinguishable from each other and from the ground wave. The method works most effectively for energetic intracloud events, because the field change pulses are powerful, isolated, and short in duration.

Figure 3.

In the previous work described by Smith [1998] and Smith *et al.* [1999b], ionospheric reflections were manually identified to determine the delay times between groundwave pulses and subsequent skywave reflections. Also, flat-earth geometry was assumed in order to simplify source and ionosphere height determinations. For the purpose of

the work described in this paper, an ionospheric-reflection model from Volland [1995] was incorporated to assure a consistent, quantitative method for determining both the reflection delays and the reflected waveform for automatic identification.

Volland [1995] developed a methodology for determining the transfer function of a longwave-spheric through the earth-ionosphere waveguide given the ground conductivity, an effective ionospheric conductivity, and the appropriate angles of ionosphere/earth incidence. The ground and ionosphere effective conductivities were assumed to be 5.0×10^{-4} and 2.2×10^{-6} S/m respectively [Volland, 1995; Wait and Spies, 1974; Field *et al.*, 1985]. The transfer function of the vertical electric field for multi-hop paths is a complex function of frequency with dependence on the geometry of the earth-ionosphere cavity and the effective conductivity of the earth and ionosphere. The transfer function accurately models the observed reflected wave, including the leading-edge polarity reversal at given distances.

Figure 4.

Skywave modeling and cross correlation are illustrated in Figure 4. The pictured event is from August 22, 1999 02:47:49.797 and was recorded by the Tampa, Florida station at a range of 269 km. For the routine processing of NBEs, the ground and first reflected sky waves are temporally distinct in the LASA electric-field-change record. The time scales of Panels 1, 3, and 4 all have the same zero-reference time, while Panel 2 does not have any propagation delay included, so the zero-reference time is arbitrary. Panel 1 of the figure shows a zoom view of an EIC pulse on a time scale of $\pm 120 \mu\text{s}$. The groundwave pulse was windowed with a 64-point Hanning window centered 6 points to the right of the trigger point, in order to minimize detrimental effects of noise and

isolate the groundwave waveform from the rest of the record prior to modeling. Panel 2 shows the Volland-model generated skywave reflection (note the reduced amplitude scale compared to the groundwave) using the previously mentioned conductivities, and the ionosphere incidence angle (calculated from the known range to the source).

Panel 3 shows a longer excerpt of the raw spheric waveform that includes both the groundwave pulse shown in Panel 1 and the skywave pulses (at delays of ~ 140 and $\sim 175 \mu s$ respectively). Panel 4 shows the result of cross correlation of the modeled skywave pulse (Panel 2) with the Panel 2 spheric waveform. Note that two cross correlation peaks appear at the approximate times of the skywave pulses. The times of the peaks (indicated by asterisks) are the best estimates of the pulse times of arrival.

All computations were performed under the assumption of spherical-earth propagation geometry. The path-length difference, d_i , between the groundwave and direct 1-hop ionospheric reflection is

$$d_i = \sqrt{(r_E + h_i)^2 + (r_E + h_s)^2 - 2(r_E + h_i)(r_E + h_s) \cos \phi_1} + \sqrt{(r_E + h_i)^2 + r_E^2 - 2(r_E + h_i)r_E \cos \phi_2} - d$$

where d is the arc-distance between the source and the receiver, r_E is the earth radius, h_i and h_s are the ionosphere and source heights, ϕ_1 is the angle subtended by the ray-path between the source and the ionospheric-reflection point (measured from the center of the earth), and ϕ_2 is the geo-centric angle subtended by the ionosphere-reflection point to the receiver. Similarly, the path-length difference between the groundwave and the

ground-ionosphere 1-hop reflection, d_{gi} , is

$$d_{gi} = \sqrt{(r_E + h_s)^2 + r_E^2 - 2(r_E + h_s)r_E \cos \phi_3} + \\ 2\sqrt{(r_E + h_i)^2 + r_E^2 - 2(r_E + h_i)r_E \cos \phi_4} - d$$

where ϕ_3 is the geo-centric angle subtended by the ray path between the source and the ground-reflection and ϕ_4 is the geo-centric angle subtended by the ground-reflection and ionospheric-reflection point (and also the ionospheric-reflection point to the receiver).

Using the two lag-times determined by the cross-correlation of the Volland-model output, the source and ionosphere heights are computed using minimum mean square error techniques as implemented via the amoeba algorithm presented by Press *et al.* [1992].

Processing of spheric waveforms proceeded automatically in this fashion for all events identified as EICs (using pulse duration and isolation criteria described by Smith *et al.* [2002]). Software was written to window and cross correlate data and then perform twin peak detection on the correlated output. A number of criteria were implemented to assure that only waveforms with a high confidence in the skywave delay estimates were passed on to the height determination routine. Among the criteria were limits on the minimum cross-correlation values, minimum signal-to-noise ratios, and maximum widths of both correlation peaks, as well as a limit on the maximum separation between the peaks. Waveforms that passed these criteria had their delays passed to the next step in LASA processing, which was determination of the source and ionosphere heights given the delays between the groundwave and skywave pulses.

Each event in the LASA database of located lightning discharges is associated with at least three waveforms recorded by different stations, since that is the minimum number of sensors required for making a two-dimensional (latitude and longitude) location determination. The analyses described in this section were performed on each waveform recorded for each event. In cases for which multiple waveforms resulted in height estimates, the mean height from all waveforms was used to represent the event height.

VLF/LF Source Height Results

Figure 5.

Source heights were determined for $\sim 100,000$ EICs recorded by LASA from April 1998 to December 2001. All of these events were associated with narrow positive or narrow negative bipolar field change pulses as identified by automatic array processing software. The ratio of positives to negatives was approximately 58:42. Source heights were found to follow a bimodal distribution that correlated well with event polarity. Figure 5 shows histograms of source height for positive-polarity and negative-polarity EICs for all events in the LASA sferic database. The median heights for positives and negatives were 13 km above ground level (AGL) and 18 km AGL respectively. Note that the heights are given as AGL. In the geometry described earlier, all stations and earth reflection points were assumed to have the same elevation (on a spherical earth with a radius of 6370 km). This is a reasonable assumption for the events occurring near Florida, where the maximum elevation is <200 m above mean sea level (MSL). The assumption is not as good in New Mexico and Colorado, where station elevations

were as high as 2250 m. For these events it may be necessary to add up to ~ 2 km to heights to obtain MSL values. However, the vast majority of events were recorded in the vicinity of Florida.

VLF/LF Ionosphere Heights

Figure 6.

Virtual ionosphere heights determined using the methods described earlier were generally in the range of 60 to 95 km. A scatter plot of ionosphere height as a function of local time of day (at the source location) is shown in Figure 6. The plot clearly shows diurnal variations between ~ 86 km during the night and ~ 70 km during the day. These values agree well with previous studies of the virtual ionospheric reflection height as a function of time of the day [Belrose, 1964]. The ionosphere height decreases during the day due to solar extreme ultraviolet photons which ionize atomic oxygen in the upper atmosphere, increasing the total ionization.

The techniques used to determine both the ionosphere heights and intracloud lightning source heights are validated by the clear diurnal variations in ionosphere height. Additionally the range in ionosphere heights for a given time of day (90% of events following within ± 2 km of the mean) implies that the uncertainty in source heights is no greater than ± 2 km. The uncertainty in the determined height is actually less than 2 km, because the observed range in ionosphere height for a given local time results from both physical day-to-day variation of the ionospheric height as well as uncertainty associated with the method.

FORTE RF System

Background

The FORTE satellite was launched Aug. 1997 with instrumentation capable of making both radio frequency (RF) [Jacobson *et al.*, 1999] and optical [Light *et al.*, 2001; Suszcynsky *et al.*, 2000] observations of lightning. The orbit altitude is approximately 820 km at an inclination of 70° , providing at most ~ 15 minutes coverage of any ground spot. The FORTE RF payload consists of two tunable receivers with 22 MHz bandwidths and one tunable 85 MHz bandwidth receiver. The FORTE radio systems and typical observations are described by Jacobson *et al.* [1999]. The FORTE optical package consists of a fast, non-imaging photometer and a slower CCD array. The FORTE satellite has collected over 4 million VHF waveforms since its launch in August 1997.

VHF Source Height Methodology

Figure 7.

For a favorable FORTE-source geometry (as illustrated in Fig. 2), intra-cloud lightning events produce RF pulse pairs (separated temporally by as much as $120 \mu\text{s}$) from the direct and ground-reflected propagation paths, as illustrated in Figure 7. These pairs are called Trans-Ionospheric Pulse Pairs (TIPPs). The FORTE RF data are processed on the ground by applying spectral whitening (to remove anthropogenic noise, such as radio and television transmissions) and de-chirping (to remove ionospheric propagation effects). Given a two dimensional geolocation and knowledge of FORTE's

location, the source height can be determined from the delay between the pulses, as described by Jacobson *et al.* [1999]. Figure 7 presents 8 ms of low-band data from October 4, 2000 at 09:17:07.297. Panel 1 presents a plot of the 8 ms FORTE RF electric field squared record. Three intense pulses of radiation from the onset of the stepped leader are apparent at 1.6 - 2.1 ms. The return stroke occurs at approximately 6.8 ms. Panel 2 presents the FORTE record for the three leader pulses and indicates the FORTE determined heights. Two similar examples of the determination of intra-cloud heights using the pulse separation method are presented by Heavner *et al.* [2002]. Possible sources of error include errors in the two-dimension lightning location, uncertainties in the FORTE location, and errors in the determination of the FORTE RF peak separation. Emprically, altitude errors resulting from the pulse separation method of altitude determination from the FORTE RF records are less than 10%.

VHF Source Height Results

Figure 8.

As previously described, the FORTE RF data analysis is often supplemented by an additional data set that provides the two-dimensional geographic location of lightning flashes. Supplementary datasets including LASA (Edot), the U.K. Meteorological sferic array [Lee, 1989], the National Lightning Detection Network [Cummins *et al.*, 1998], and the FORTE Lightning Location System (LLS) [Suszcynsky *et al.*, 2001]. Figure 8 shows a histogram of FORTE determined TIPP heights based on locations provided by the above four systems. FORTE does not distinguish polarity of the TIPPs. The lower altitude TIPPS identified through UKMet and LASA (Edot) coincidences appear to be

statistically significant.

Joint Sferic Array/FORTE Results

Figure 9.

The sferic array was originally deployed to support FORTE satellite operations by providing ground truth for lightning discharges. Of the more than 100,000 events in the LASA database with source height estimates, 335 were also recorded by FORTE. Of these events, approximately 100 had independent FORTE height estimates. Figure 9 shows a scatter plot of the LASA heights versus FORTE heights, with positive-polarity events (as identified by LASA) represented as red ‘+’ symbols and negative-polarity events represented as green ‘Δ’ symbols. The source height determinations from the two platforms are in good agreement, but with a +1.0 km average bias for the LASA-derived source heights. Ignoring the bias, 90% of the LASA heights agree within ± 1.0 km of the FORTE heights. We place higher confidence in the FORTE height determinations because the observation geometry is simpler and because the higher frequency radio signals are more closely represented by the geometrical optics assumed by the height determination methods. The outliers in Figure 9 (especially the events with LASA source heights >25 km) are believed to be poor height determinations that slipped through the quality control criteria implemented in LASA automatic processing.

Summary and Conclusion

During the 4+ years of LASA observations described in this paper, over one million EICs were detected and located by the array. Using methods developed from those

introduced by Smith [1998] and Smith *et al.* [1999b], source heights were determined for over 100,000 of these events with both positive and negative polarities.

Positive- and negative-polarity EICs occurred in distinctive altitude regimes with positives occurring between 7 and 15 km AGL and negatives occurring between 15 and 20 km. The distinctness of the two peaks shown in Figure 5 suggests that the charge regions responsible for the discharges occur at fairly uniform altitudes over time and location. Furthermore, the polarities of the discharges suggest that the region between the peaks, around 15 km, is a region of positive charge. Although this may not be the case for all thunderstorms, it does appear to be the case for EIC-producing thunderstorms. The majority of the events contributing to this study were from the Florida area.

Ionosphere virtual heights determined using the methods introduced in this paper followed a strict diurnal variation that was consistent with previously published ionosphere heights at VLF/LF frequencies. The agreement with previous observations provides validation for the method. The limited range of ionosphere heights for a given time of day suggests that uncertainties associated with the method are smaller than 2 km.

VHF radio receivers on the FORTE satellite provided independent height estimates for 100 of the LASA-recorded EIC events. The heights determined by the two methods were in good agreement with LASA reporting heights that were on average 1.0 km higher than the FORTE heights. With higher confidence ascribed to the FORTE height determination method, the bias is believed to be associated with the LASA height

determination technique. Thus heights presented throughout this paper should be reduced by 1 km in order to be consistent with the FORTE results. The good agreement (generally within 1 km after removal of the bias) between the two techniques suggests that both provide a valid means of determining the heights of intracloud lightning discharges.

Acknowledgments. This work was performed under the auspices of the United States Department of Energy. LANL personnel who also made significant contributions include M Carter, D Roussel-Dupré, M Pongratz, M Eberle, and A Waldrum. We thank the following individuals and institutions who have hosted LANL Sferic Array stations: T Hamlin, J Harlin, P Krehbiel, B Rison, M Stanley, and R Thomas of NM Tech; R Griego, J King, D Klassen, and H Pleasant of Eastern NM Univ.; J Morgan of Mesa Tech. College; D Morss and B Strabley of Creighton Univ.; M Brooks, J Madura, and F Merceret of NASA KSC; R Chang, D Rabson, and D Spurgin of the Univ. of South FL; Walter, Leslie, and Cheryl Peterson of Cyberstreet in Fort Myers; P Hackett, T Kelly, S Morgera, V Ungvichian, and H Vasant of FL Atlantic Univ.; J Goetten, V Rakov, K Rambo, and M Uman of the Univ. of FL; S Patterson and T Trost of Texas Tech Univ.; G McHarg, K Broome, and D Vititoe of the U.S. Air Force Academy; R Olson of Plains Network; J Fulton of Plains Telephone; and W Petersen, S Rutledge, and W Naylor of Colorado State Univ; D Rabson and P Mukherjee of Univ. S. FL; L Jones and J Park of Univ. Central FL; and J Olivero and D Burke of Embry Riddle Aero. Univ. M Heavner acknowledges many fruitful discussions with C Talus.

References

- Belrose, J. S., *Propagation of radio waves at frequencies below 300 kc/s*, chapter Present knowledge of the lowest ionosphere, p. 3. Macmillan Co, 1964.
- Cummins, K. L., M. J. Murphy, E. A. Bardo, W. L. Hiscox, R. B. Pyle, and A. E. Pifer, A combined TOA/MDF technology upgrade of the U.S. National Lightning Detection Network, *J. Geophys. Res.*, *103*(D8), 9035–9044, 1998.
- Field, E. C., J. L. Heckscher, P. A. Kossey, and E. A. Lewis, *Handbook of Geophysics and the Space Environment*, chapter 10.2 Some aspects of Long Wave Propagation. Air Force Geophysics Laboratory, 1985.
- Heavner, M. J., D. A. Smith, A. R. Jacobson, and R. J. Sheldon, LF/VLF and VHF lightning fast stepped leader observations, *J. Geophys. Res.*, 2002, accepted.
- Holden, D. N., C. P. Munson, and J. C. Devenport, Satellite observations of transionospheric pulse pairs, *Geophys. Res. Let.*, *22*(8), 889–892, 1995.
- Jacobson, A. and X. Shao, Using geomagnetic birefringence to locate sources of impulsive, terrestrial VHF signals detected by satellites on orbit, *Radio Science*, *36*(4), 671–680, 2001.
- Jacobson, A. R. and T. E. L. Light, Bimodal radiofrequency pulse distribution of intracloud-lightning signals recorded by the forte satellite, *J. Geophys. Res.*, 2002, submitted.
- Jacobson, A. R., S. O. Knox, R. Franz, and D. C. Enemark, FORTE observations of lightning radio-frequency signatures: Capabilities and basic results, *Radio Sci.*, *34*(2), 337–354, 1999.

- Jacobson, A. R., K. L. Cummins, M. Carter, P. Klingner, D. Roussel-Dupré, and S. O. Knox, FORTE radio-frequency observations of lightning strokes detected by the National Lightning Detection Network, *J. Geophys. Res.*, 105(D12), 15,653–15,662, 2000.
- Kinzer, G., Cloud-to-ground lightning versus radar reflectivity in Oklahoma thunderstorms, *Journal Of The Atmospheric Sciences*, 31(3), 787–799, 1974.
- Krider, E., G. Radda, and R. Noggle, Regular radiation field pulses produced by intracloud lightning discharges, *J. Geophys. Res.*, 80(27), 3801–4, 1975.
- Lee, A. C. L., Ground truth confirmation and theoretical limits of an experimental VLF arrival time difference lightning flash locating system, *Quarterly Journal Of The Royal Meteorological Society*, 115(489), 1147–1166, 1989.
- LeVine, D. M., Sources of the strongest RF radiation from lightning, *J. Geophys. Res.*, 85, 4091–4095, 1980.
- Light, T. E., D. M. Suszcynsky, and A. R. Jacobson, Coincident radio frequency and optical emissions from lightning, observed with the FORTE satellite, *J. Geophys. Res.*, 106(22), 28223–28231, 2001.
- Massey, R. and D. Holden, Phenomenology of transionospheric pulse pairs, *Radio Science*, 30(5), 1645–1659, 1995.
- Massey, R. S., S. O. Knox, R. C. Franz, D. N. Holden, and C. T. Rhodes, Measurements of transionospheric radio propagation parameters using the FORTE satellite, *Radio Science*, 33(6), 1739–1753, 1998.
- McDonald, T., M. Uman, J. Tiller, and W. Beasley, Lightning location and lower-ionospheric

- height determination from 2-station magnetic-field measurements, *Journal Of Geophysical Research-Oceans And Atmospheres*, 84(C4), 1727–1734, 1979.
- Medelius, P. J., E. M. Thomson, and J. S. Pierce, E and DE/DT waveshapes for narrow bipolar pulses in intracloud lightning, in *Proceedings of the International Aerospace and Ground Conference on Lightning and Static Electricity*, pp. 12–1 to 12–10. 1991, NASA/CP-3106.
- Press, W. H., S. A. Teukolsky, W. T. Betterling, and B. P. Flannery, *Numerical Recipes in C*. Cambridge University Press, 2 edition, 1992.
- Rison, W., R. J. Thomas, P. R. Krehbiel, T. Hamlin, and J. Harlin, A GPS-based three-dimensional lightning mapping system: Initial observations in central New Mexico, *Geophys. Res. Let.*, 26, 3573–3576, 1999.
- Smith, D. A., *Compact intracloud discharges*, Ph.D. thesis, Univ. of Colorado, Boulder, 1998.
- Smith, D. A., X. M. Shao, D. N. Holden, C. T. Rhodes, M. Brook, P. R. Krehbiel, M. Stanley, W. Rison, and R. J. Thomas, A distinct class of isolated intracloud lightning discharges and their associated radio emissions, *J. Geophys. Res.*, 104(D4), 4189–4212, 1999a.
- Smith, D. A., R. S. Massey, K. C. Wiens, K. B. Eack, X. M. Shao, D. N. Holden, and P. E. Argo, Observations and inferred physical characteristics of compact intracloud discharges, in H. Christian (ed.), *Proceedings of the 11th International Conference on Atmospheric Electricity*, pp. 6–9. 1999b, NASA/CP-1999-209261.
- Smith, D. A., K. B. Eack, J. Harlin, M. J. Heavner, A. R. Jacobson, R. S. Massey, X. M. Shao, and K. C. Wiens, The Los Alamos Sferic Array: A research tool for lightning investigations, *J. Geophys. Res.*, 107(D13), 10.1029/2001JD000502, 2002.

- Suszcynsky, D., T. Light, S. Davis, J. Green, J. Guillen, and W. Myre, Coordinated observations of optical lightning from space using the FORTE photodiode detector and CCD imager, *J. Geophys. Res.*, *106*(D16), 17897–17906, 2001.
- Suszcynsky, D. M., M. W. Kirkland, A. R. Jacobson, R. C. Franz, S. O. Knox, J. Guillen, and J. L. Green, FORTE observations of simultaneous VHF and optical emissions from lightning: Basic phenomenology, *J. Geophys. Res.*, *105*(D2), 2191–2201, 2000.
- Volland, H., *Atmospheric Electrodynamics*, volume 2, chapter Longwave Sferics Propagation within the Atmospheric Waveguide, pp. 65–93. CRC Press, 1995.
- Wait, J. and K. Spies, Magneto-telluric fields for a segmented overburden, *Journal Of Geomagnetism And Geoelectricity*, *26*(5), 449–458, 1974.
- Willett, J. C., J. C. Bailey, and E. P. Krider, A class of unusual lightning electric field waveforms with very strong high-frequency radiation, *J. Geophys. Res.*, *94*, 16255–16267, 1989.

DA Smith, Space and Atmospheric Sciences Group, NIS-1, MS D466, Los Alamos National Laboratory, Los Alamos NM 87545. smithda@lanl.gov

Received 2002/09/25

This article will appear in Radio Science.

This manuscript was prepared with AGU's L^AT_EX macros v5, with the extension package 'AGU++' by P. W. Daly, version 1.6b from 1999/08/19.

Figure Captions

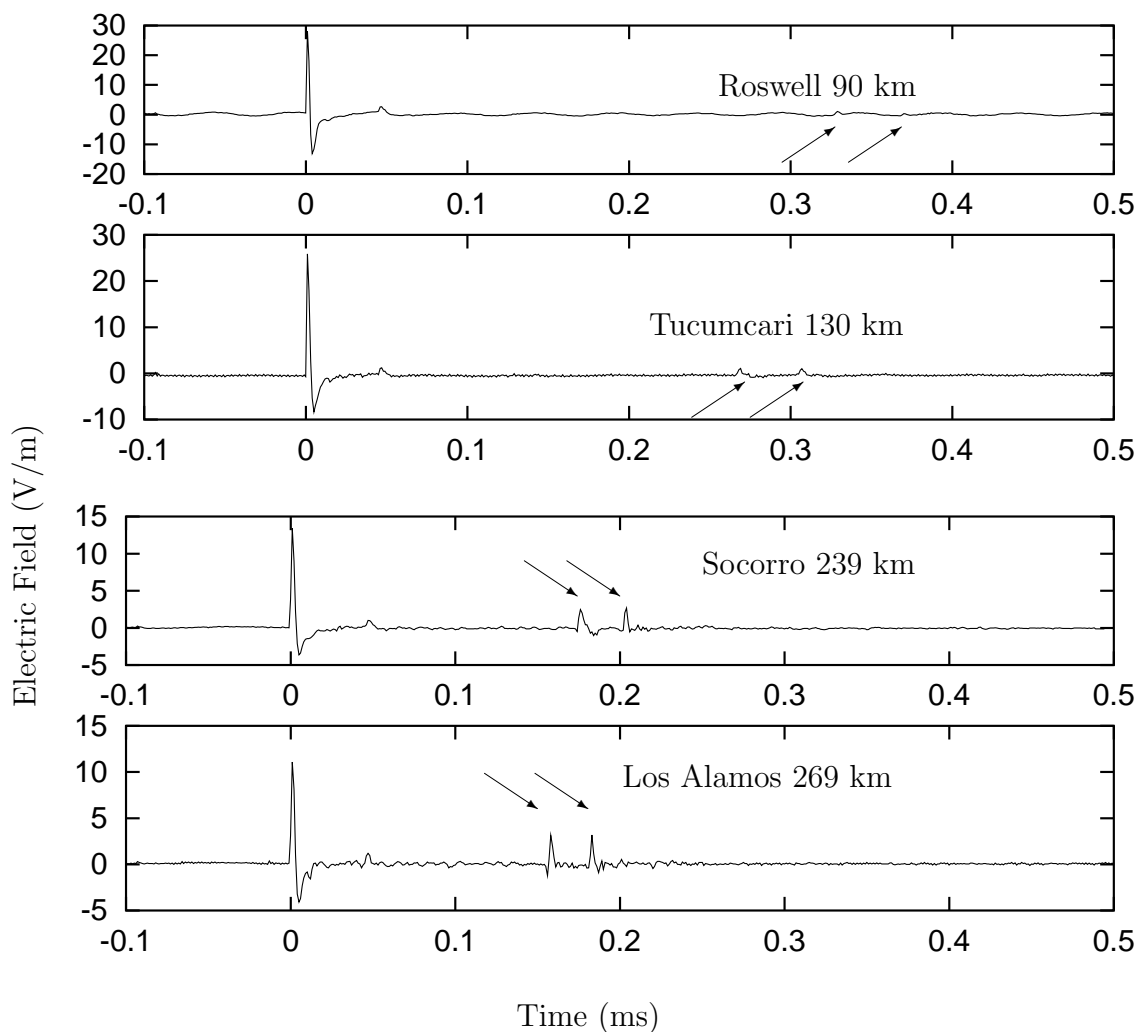


Figure 1. A 4 station sferic array observation of a NPBP at 04:47:27.085323 on September 30, 1999. The names of the four recording stations are shown on the waveform plots. The great circle distance between the sferic array determined location and each station is indicated. The ionosphere and ground-ionosphere reflected pulses are indicated by small arrows. Note the polarity reversal between the near stations and Los Alamos. At farther distances from the source, the reflections undergo quasi-Brewster angle effects by the ionospheric reflection which cause the polarity reversal.

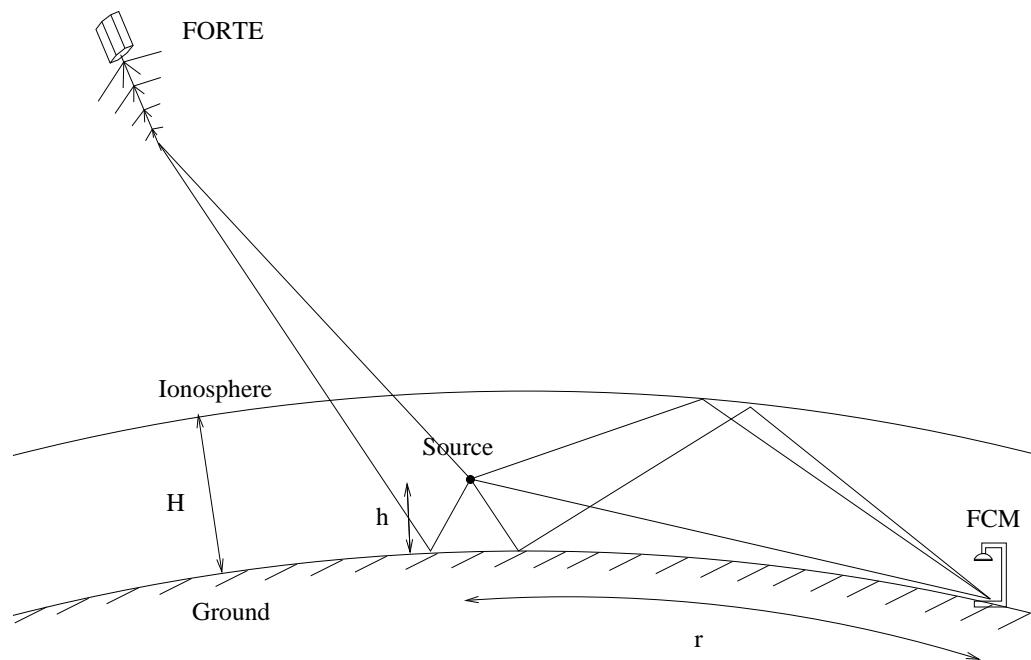


Figure 2. The direct, ionosphere reflection, and ground-ionosphere reflection paths for an intra-cloud pulse to a spheric array electric field change meter (FCM) station are illustrated. The FORTE direct and ground-reflection geometries are also indicated.

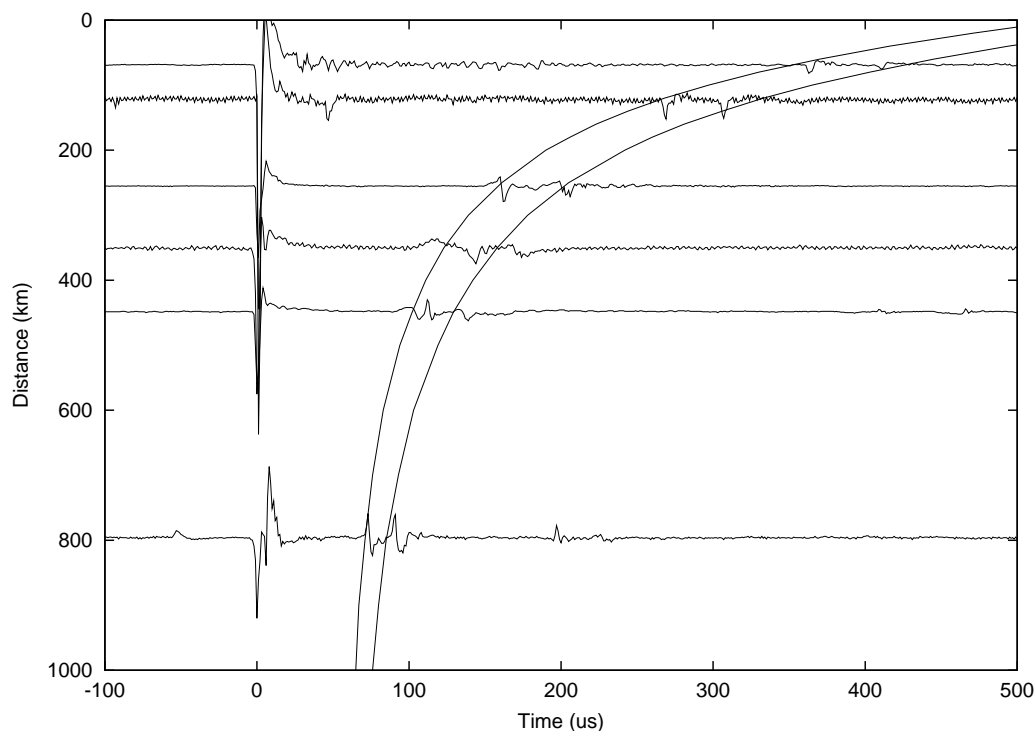


Figure 3. This figure illustrates the effect of distance from source on delay of reflected pulses. The two curved lines are the theoretical curved-earth delays for the ionosphere and ground-ionosphere pulses for a source at 12 km altitude and an ionospheric virtual height of 86 km. The waveforms are from multiple NNBPs which had source and ionospheric heights within ± 1 km of 12 km and 86 km, respectively. The amplitudes of the electric-field waveforms are arbitrarily scaled for display purposes. Note that two-hop ionospheric-reflections are also apparent in the two most distant waveforms.

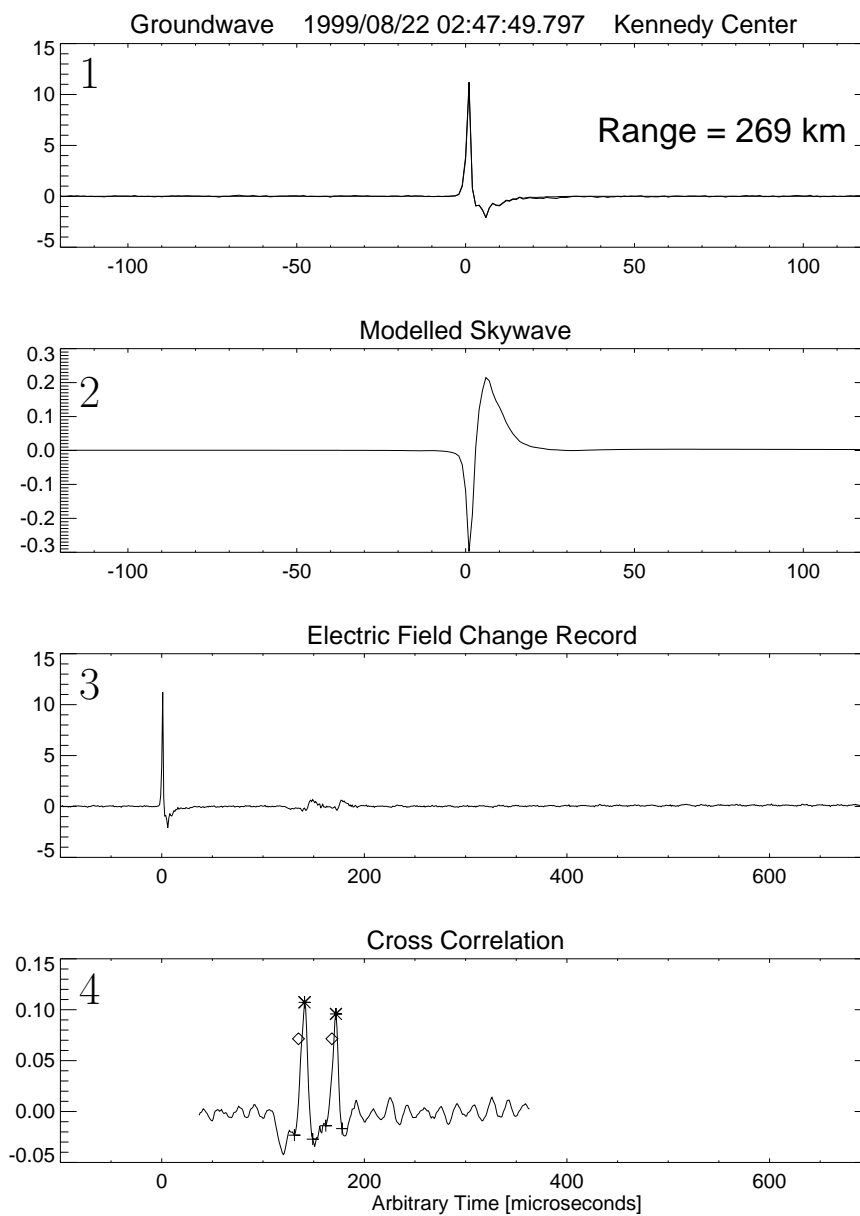


Figure 4. An illustration of the method for determining the ionosphere and ground-ionosphere reflection delays. Panel 1 is a plot of the windowed groundwave portion of the electric field change record. Panel 2 shows the skywave output of the Volland model (with an arbitrary time offset). Panel 3 is a plot of an $800 \mu\text{s}$ portion of the electric field change record. Panel 4 presents the cross correlation of the model skywave with the data. The first and second peaks in the cross correlation (indicated by asterisks) correspond to the time-tagged skywave pulses.

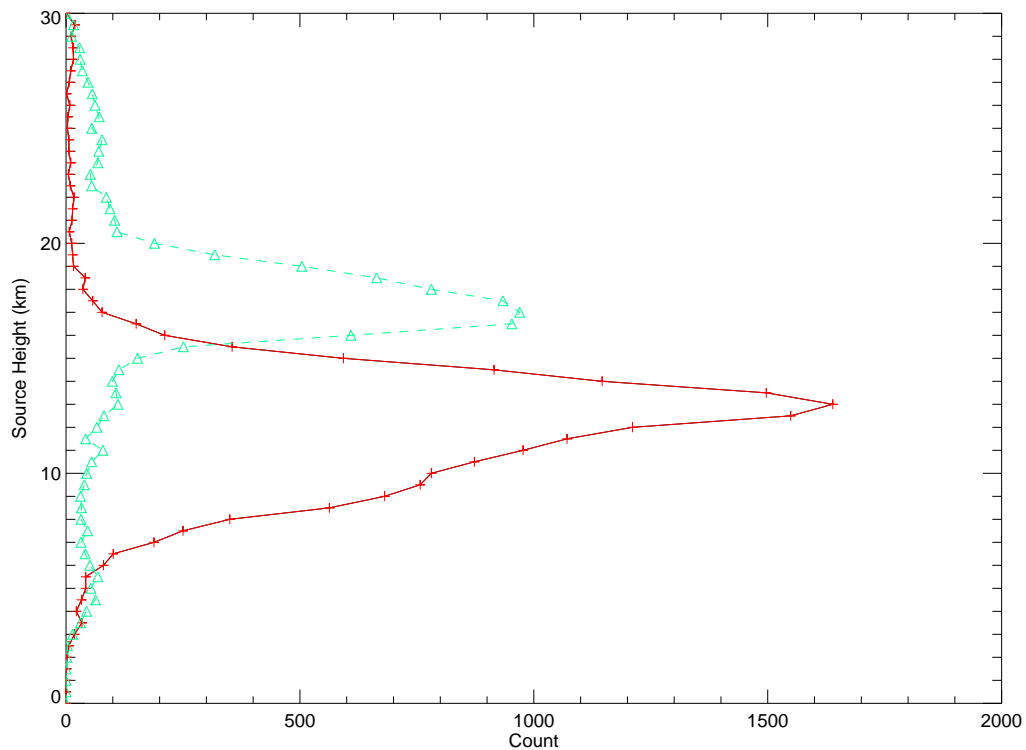


Figure 5. Histogram of energetic intra-cloud event heights as determined by the spheric array. The red solid curve (with ‘+’ symbols) is the positive EIC distribution and the green dashed curve (with ‘ Δ ’ symbols) is the negative EIC distribution. A total of 115,537 event heights are plotted in .5 km bins.

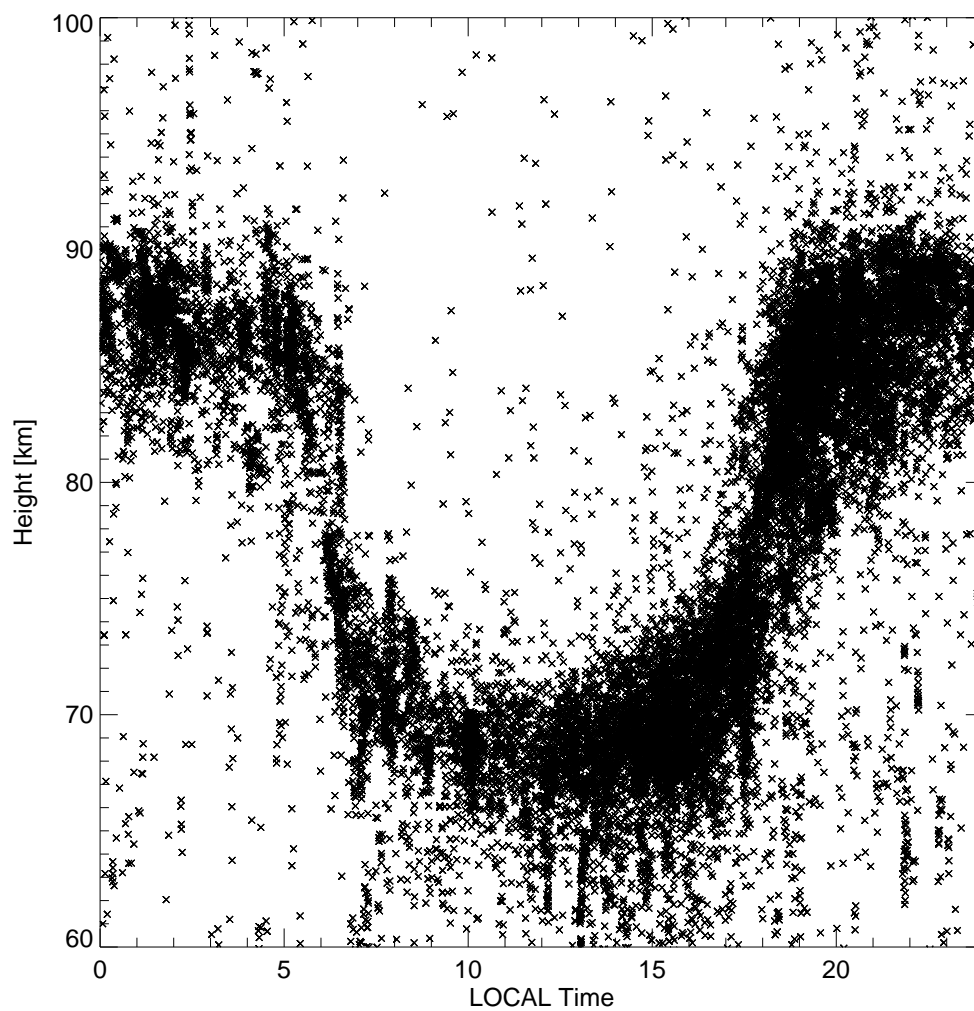


Figure 6. A scatter plot of the ionospheric virtual height as a function of local time shows a clear diurnal variation. The times and heights correspond well to previous ionospheric height observations, increasing confidence in the method described in this paper.

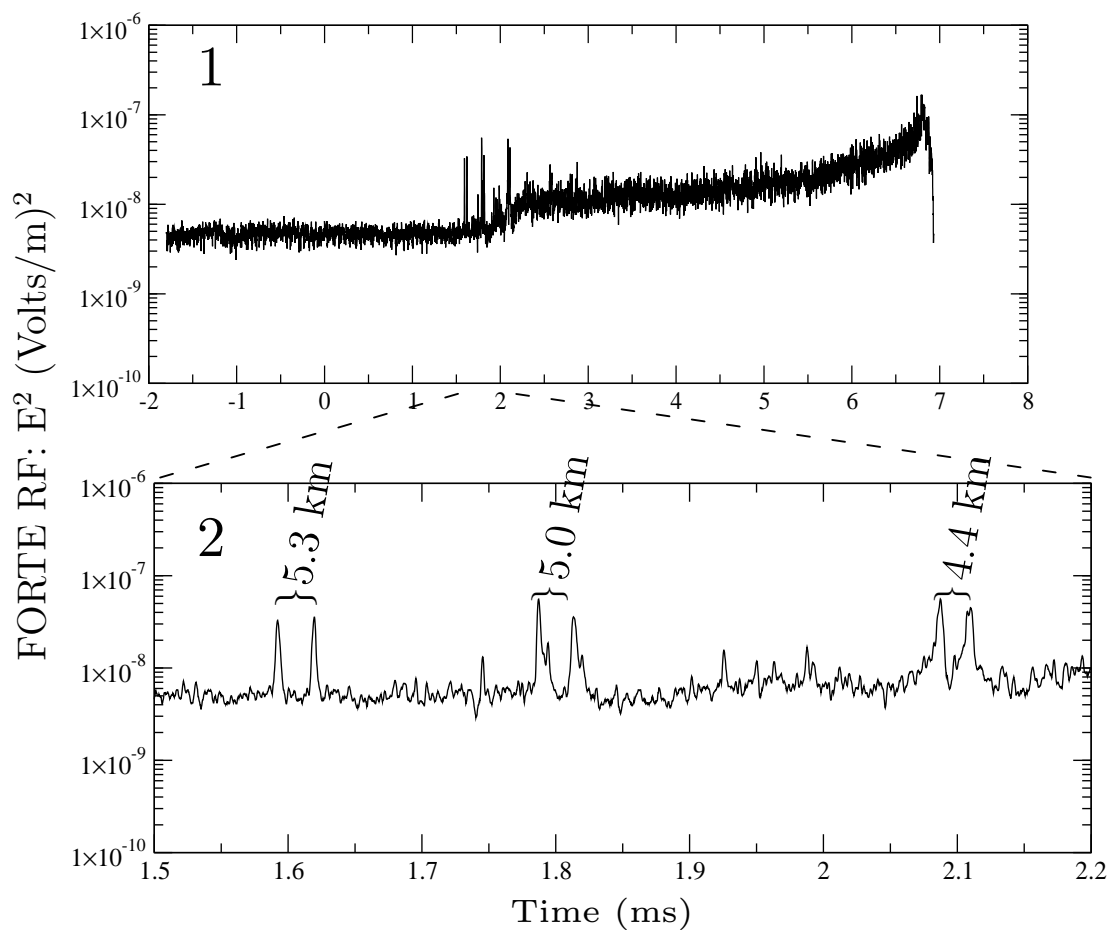


Figure 7. This example of a FORTE leader and return stroke observation illustrates the altitude determination of FORTE for pulse pairs. Panel 1 is an 8 ms FORTE RF record. The event is a return stroke with strong leader activity. This interpretation is confirmed by the LASA observations (not shown). Panel 2 shows a plot of a temporal zoom around the FORTE TIPP's. The FORTE heights determined based on the LASA return stroke location and the separation between the pulse pairs are shown. The descending leader steps provide confidence in the FORTE method.

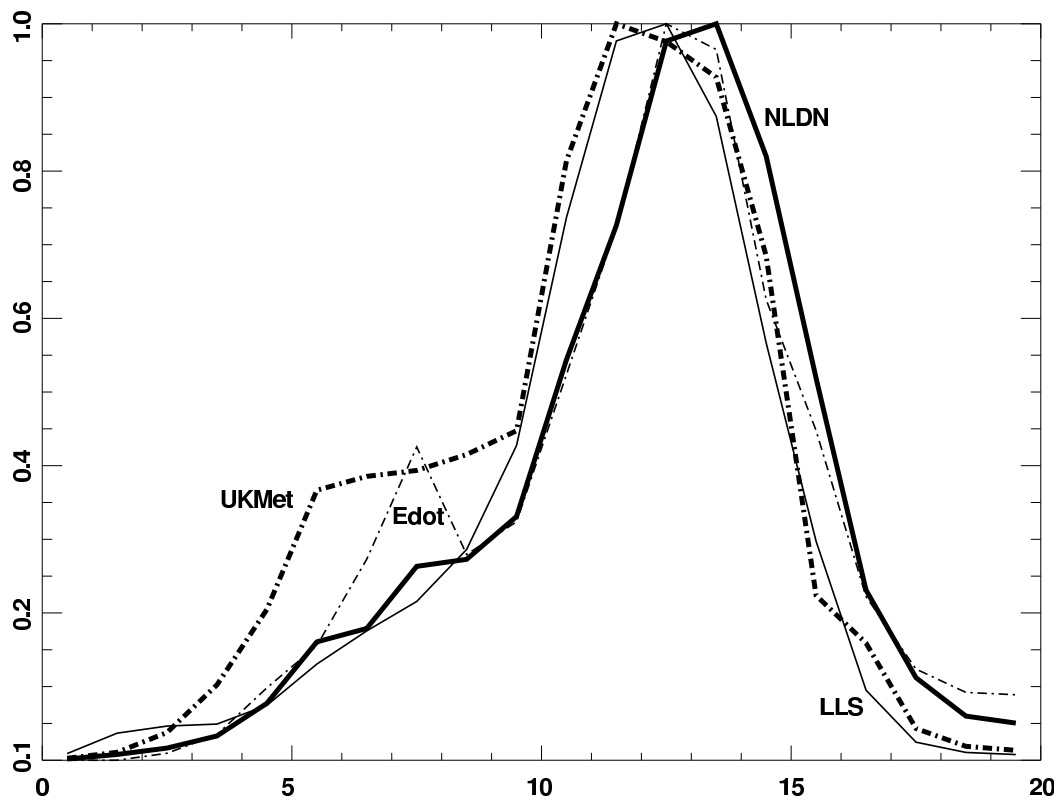


Figure 8. Relative histograms of FORTE determined EIC heights. The four different systems (UKMet, LASA (Edot), NLDN, and LLS) used to provide the lightning locations result in slightly different histograms, but are in good overall agreement.

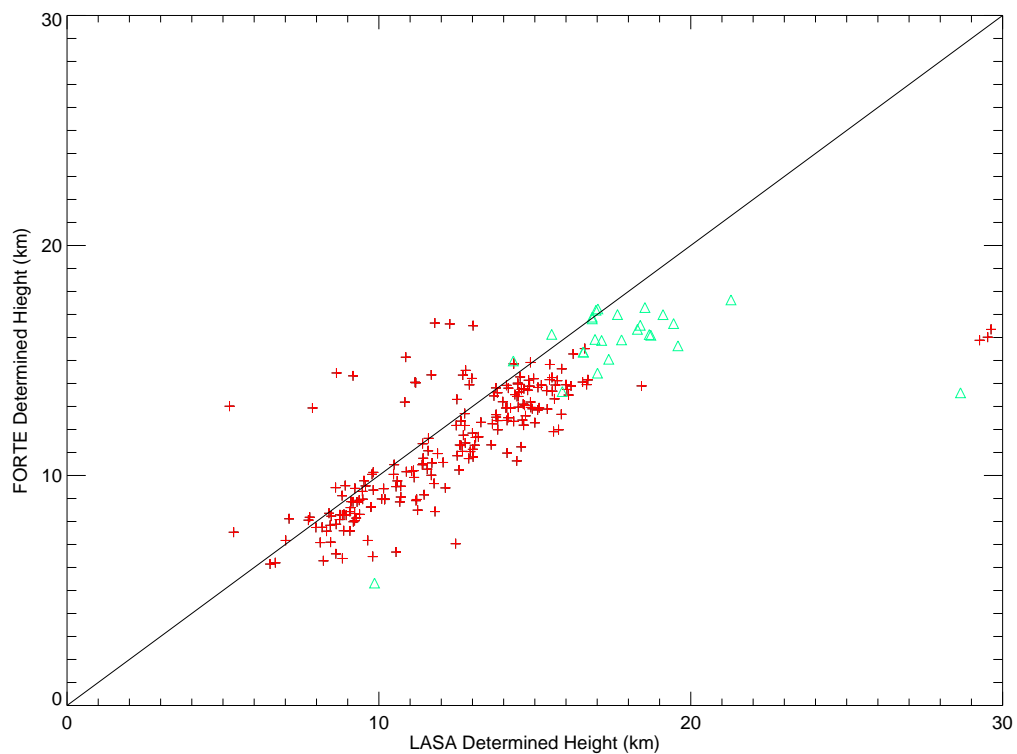


Figure 9. A scatter plot of LASA and FORTE-determined EIC heights. The line plotted shows the case for perfect agreement between the two systems. Positive EICs are plotted as red '+' symbols and Negative EICs are plotted as green triangles.